Comparison of fatigue crack growth of riveted and bonded aircraft lap joints made of Aluminium alloy 2024-T3 substrates – A numerical study

2017 J. Phys.: Conf. Ser. 843 012035

(http://iopscience.iop.org/1742-6596/843/1/012035)

IOP Conf. Series: Journal of Physics: Conf. Series **843** (2017) 012035 doi:10.1088/1742-6596/843/1/012035

Comparison of fatigue crack growth of riveted and bonded aircraft lap joints made of Aluminium alloy 2024-T3 substrates – A numerical study

S Pitta[1], J I Rojas[1] and D Crespo[2]

[1] Dept. of Physics-Division of Aerospace Engineering, C/Esteve Terradas 5, Castelldefels, 08660 Spain

[2] Dept. of Physics, C/Esteve Terradas 5, Castelldefels, 08860 Spain

E-mail: siddharth.pitta@estudiant.upc.edu, josep.ignasi.rojas@upc.edu, daniel.crespo@upc.edu

Abstract. Aircraft lap joints play an important role in minimizing the operational cost of airlines. Hence, airlines pay more attention to these technologies to improve efficiency. Namely, a major time consuming and costly process is maintenance of aircraft between the flights, for instance, to detect early formation of cracks, monitoring crack growth, and fixing the corresponding parts with joints, if necessary. This work is focused on the study of repairs of cracked aluminium alloy (AA) 2024-T3 plates to regain their original strength; particularly, cracked AA 2024-T3 substrate plates repaired with doublers of AA 2024-T3 with two configurations (riveted and with adhesive bonding) are analysed. The fatigue life of the substrate plates with cracks of 1, 2, 5, 10 and 12.7mm is computed using Fracture Analysis 3D (FRANC3D) tool. The stress intensity factors for the repaired AA 2024-T3 plates are computed for different crack lengths and compared using commercial FEA tool ABAQUS. The results for the bonded repairs showed significantly lower stress intensity factors compared with the riveted repairs. This improves the overall fatigue life of the bonded joint.

Keywords: Fatigue, stress intensity factor, finite element analysis, crack, joint, repair

1. Introduction

Aircraft structures are made of many small parts, assembled to form major structures. Most of the aircraft skin is made of aluminium alloys and composites. During the operation of the aircraft, structures are subjected to static and dynamic loading. A safety factor of 1.5 is incorporated in the design of aircraft structures, so to prevent the structure from failing under static loading. On the other side, metals have tendency to form fatigue cracks due to repetitive loading that can be of tensile, torsion or vibrational nature. Hence, fatigue of aircraft structures must be well-understood to prevent accidents because the majority of catastrophic failures of aerospace parts occur due to cyclic loading during the aircraft service life. Early detection of cracks in the structure allows calculating the expected life of the part before failure and hence it can be repaired at critical size to prevent final failure.

The common repair options for cracked metal plates are patches or doublers joined with mechanical fasteners and adhesive bonding. Rivets are also widely used in aircrafts to join the skin panels. The fastened joint strength depends on various parameters such as rivet diameter, material properties, fastening pattern and clamping force [1-3]. Riveting of the joints induces residual stresses in the substrate plates, and the residual stresses are directly proportional to rivet squeeze force. A major disadvantage of riveted joints are the holes created in the plate as

they cause high stress concentrations. Cold expansion [4], clamping force [5] and interference fit [6] can reduce the stress concentrations around the fastened holes, improving the fatigue life. Iyer *et al.* [7] investigated the fatigue behaviour of single and double self-piercing rivets with experiments and finite element methods. Rijck *et al.* [8] investigated the implications of rivet driven head dimensions on the fatigue performance of aircraft lap joints. Skorupa *et al.* [9] investigated fatigue life and fatigue crack location in riveted aircraft lap joints in fuselage. Esmaeili *et al.* [10] investigated the effects of torque tightening on fatigue strength of aluminium alloy (AA) 2024-T3 double-lap bolted joints. Carter *et al.* [11] investigated on production quality of aircraft fastener holes on fatigue life. Their investigation showed that machining of fastener holes has a more important effect on fatigue life than residual stresses. Fretting fatigue damage occurs when contact regions experience cyclic stresses, initiating micro crack formation and leads to failure. Fretting fatigue crack initiation in double lap bolted joints was investigated by Ferjaoui *et al.* [12]. Hojjati *et al.* [13] developed fretting fatigue crack initiation lifetime predictor tool using damage mechanics approach. Corrosion also plays an important role in fatigue life. Kermanidis *et al.* [14] investigated fatigue and damage tolerance behaviour of corroded AA 2024-T351 for different stress ratios. Corrosion of aluminium alloys is classically attributed to complex processes of oxidation [15, 16]. Investigations performed on aircraft alloys showed that corrosion is a damage process not only limited to the surface (affecting the yield strength (YS) and fatigue life through occurrences of corrosion notches or pits), but which also causes diffusion-controlled hydrogen embrittlement of the materials [17-21].

Adhesive bonding of structures is another most used technique in joining parts. In bonded joints, the stresses are distributed uniformly along the bond area, hence reducing the stress concentrations in the joint. Most of the bonded repairs on cracked metallic plates consist of bonded composite patches [22-24]. The strength of the adhesive and surface preparation play a key role on the strength of the joint and fatigue resistance [25]. Bonded composite repairs of cracked primary aircraft structures under fatigue loading were investigated by Baker [26]. Uncertainties of the material and their effect on aircraft fuselage fatigue life was investigated by Koutsourelakis *et al.* [27]. They proposed a cohesive element model to calculate the fatigue life of aircraft fuselages. Fatigue durability of aircraft repairs with clad AA 7075-T6 bonded joints was investigated experimentally and numerically by Harman *et al.* [28].

In this paper, the fatigue life of AA 2024-T3 is computed for different crack lengths using FRANC3D. Second, the performance of AA 2024-T3 plates repaired with mechanically fastened joints and adhesively bonded joints is compared. A three dimensional (3D) finite element model is developed in ABAQUS and imported to FRANC3D to obtain the fatigue life. Later, the repair configurations are modelled and analysed in ABAQUS to compute the stress intensity factors.

2. Materials and Methods

2.1 Materials

AA 2024-T3 is widely used in manufacturing aircraft skin panels due to its high strength and fatigue resistance properties. Table 1 and Table 2 show, respectively, the mechanical properties and chemical composition of AA 2024-T3, used for the substrate and doublers. The thickness of aircraft skin at high load areas is 3.175mm, while the doublers have thickness of

1.5875mm. The length/width of the substrate plates used in this investigation is 342.8mm/25.4mm with an aspect ratio of 13.5. The doublers have a length of 203.2mm and 152.4mm, width of 25.4mm with aspect ratios of 8 and 6. A two-part adhesive HYSOL 9480 is used for the adhesive bonding of the doublers to the cracked plates. The Young's modulus of Hysol 9480 is 4.5 GPa (ISO 527-3) and the tensile strength (TS) is 47 MPa (ISO 527-3).

Table 1 Mechanical properties of the as-received, commercial aluminium alloys (AA) 2024-T3.

Aluminium alloy	YS (MPa)	TS (MPa)	% Area Reduction	Brinell hardness
AA 2024-T3	316	464	20.2%	HB 123

Table 2 Chemical composition of the as-received, commercial aluminium alloys (AA) 2024-T3 [27].

Aluminium alloy	Units	Si	Fe	Cu	Mn	Mg	Zn	Ti	Cr	Al
AA 2024-T3	Wt. %	0.50	0.50	4.9	0.9	1.8	0.25	0.15	0.10	90.9
ASTM E8/B557	At. %	0.07	0.20	4.4	0.59	1.4	0.09	0.02	0.01	93.22

2.2 Modelling in FRANC3D

A simple 3D finite element model is modelled using FEA tool ABAQUS with material properties and boundary conditions. Pressure is applied on the ends of the substrate plates with different magnitudes of 93.6 MPa (design limit load) and 140 MPa (ultimate load) in the tensile direction. The ultimate load the joint can carry was calculated from the strength of the rivets (rivet value times number of rivets). A safety factor of 1.5 applied to the ultimate load is used to calculate the design limit load of the joints. The aluminium alloy substrate plates are modelled with solid elements of 8-node linear brick elements with reduced integration. These plates are meshed with an element size of 2mm and static general step is considered to generate the input file in ABAQUS. Then, the input file is imported to FRANC3D where cracks of 1, 2, 5, 10 and 12.7mm are induced in the centre of the model, as shown in Fig. 1(a). FRANC3D has an inbuilt meshing algorithm to mesh the crack fronts with an option to refine depending on the complexity of model. The model meshed in FRANC3D is shown in Fig. 1(b). Static analysis is performed on the cracked plate to obtain stress intensity factors at the crack fronts. The cracks are allowed to grow under quasi-static power law criterion. Based on the fatigue crack growth (FCG) for the given loads, the fatigue life of the plate is computed in FRANC3D. For this purpose, the material properties shown in Table 3 were used, together with the NASGRO version 3 equation:

$$\frac{da}{dN} = C\left[\frac{1-f}{1-R}\Delta K\right]^n \frac{\left(1-\frac{\Delta K_{th}}{\Delta K}\right)^p}{\left(1-\frac{K_{max}}{K_c}\right)^q} \quad (1)$$

where $\frac{da}{dN}$ is the crack growth rate, ΔK is the applied stress-intensity factor, R is the stress ratio, $\Delta K_{th}$is the fatigue threshold, K_{max} is the stress-intensity factor corresponding to peak applied load, K_c is the critical stress intensity, f is Newman's crack opening function, C, n, p and q are curve fitting constants.

Table 3 Material properties as used in the NASGRO version 3 equation (Eq. 1) for AA 2024-T3.

Material	TS (MPa)	YS (MPa)	K_c (MPa.mm$^{0.5}$)	C (mm/cycle)	n	p	q
AA 2024-T3	455.07	365.44	36.26	1.832e-12	3.284	0.5	1

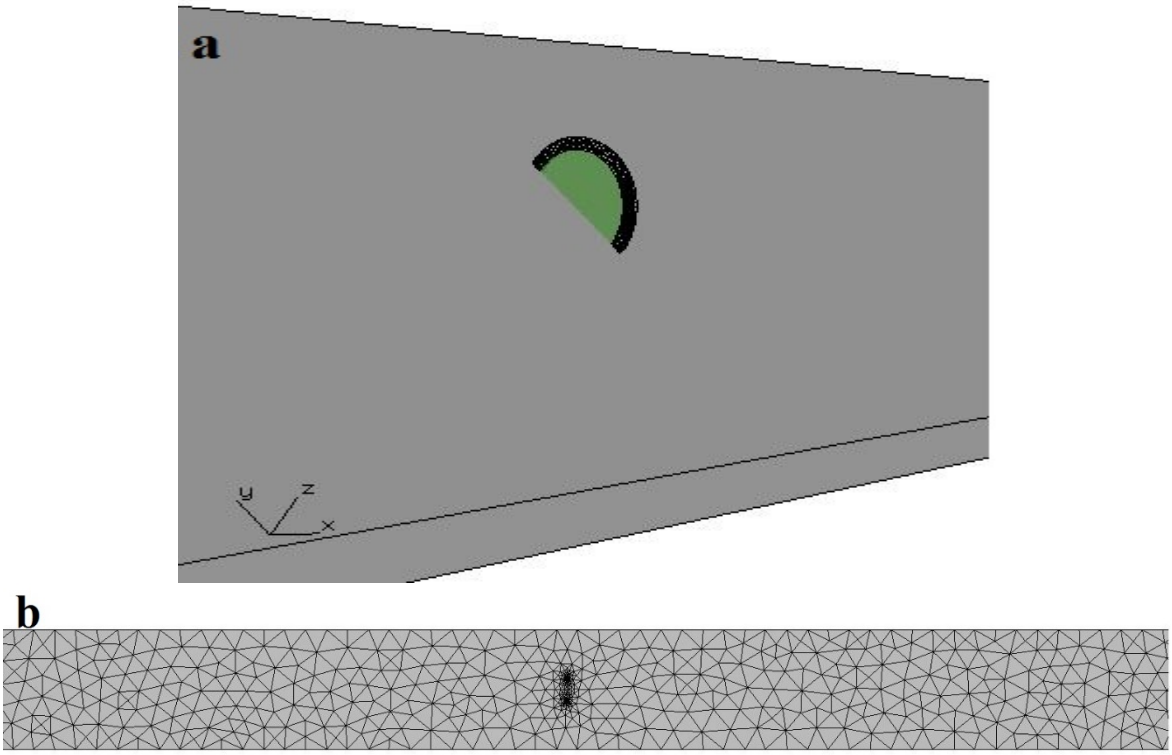

Fig. 1 (a) Isometric view of insertion of crack in the substrate plate in the graphical user interface of FRANC3D, and (b) lay out view of the mesh in the plate as generated by the FRANC3D mesh algorithm.

2.3 Modelling in ABAQUS

Cracked aluminium substrate plates are repaired with two doublers with riveted and bonded joint configuration. Models of these repairs are analysed in ABAQUS to obtain the stress intensity factors and the results study is performed for various crack lengths are compared. The aluminium alloy substrates and doublers are modelled as 3D shell elements to increase the computational efficiency. Assumption of shell elements considered in this study provides reasonable results compared with solid elements. If two dimensions of the specimen are much greater than the third dimension, then shell elements provide good results. Table 1 shows the properties as used for substrates and doublers. The rivets are modelled as point-based fasteners, as shown in Fig. 2(a). Bushing elements are considered to simulate the stiffness of the rivets in six directions. These stiffness values are calculated using the following formulae [29]:

$$K_1 = \left\{\frac{k}{m}\left[\left(\frac{t_{shell1}+t_{shell2}}{2d}\right)^{\lambda}\left(\frac{1}{E_{11,shell1}t_{shell1}}+\frac{1}{m.E_{11,shell2}t_{shell2}}+\frac{1}{2.E_{fast}t_{shell1}}+\frac{1}{2m.E_{fast}t_{shell2}}\right)\right]\right\}^{-1} \quad (2)$$

$$K_2 = \left\{\frac{k}{m}\left[\left(\frac{t_{shell1}+t_{shell2}}{2d}\right)^{\lambda}\left(\frac{1}{E_{22,shell1}t_{shell1}}+\frac{1}{m.E_{22,shell2}t_{shell2}}+\frac{1}{2.E_{fast}t_{shell1}}+\frac{1}{2m.E_{fast}t_{shell2}}\right)\right]\right\}^{-1} \quad (3)$$

$$K_3 = \frac{\pi d^2 E_{fast}}{4(t_{shell1} + t_{shell2})} \quad (4)$$

$$K_4 = K_5 = \frac{\pi d^2}{16}\left(\frac{E_{fast} d^2}{4L} + G_{fast}.L\right) \quad (5)$$

$$K_6 = \frac{G\pi d^4}{32L} \quad (6)$$

Where k is 2.2 and λ is 0.4 for solid rivet, m is 1 for single shear, t_{shell1} and t_{shell2} are thickness of shell 1 and shell 2, d is diameter of rivet hole, E_{11},E_{22},E_{fast} are elastic modulus of plates and rivet, G_{fast} is shear modulus of rivet and L is length of the fastener.

The adhesive bonding of the substrate and doublers is modelled as cohesive contact between the surfaces. The adhesive properties are mentioned Section 2.1. Traction-separation law criteria is used in modelling cohesive with parameters (*E*/*Enn*, *G1*/*Ess* and *G2*/*Ett*). These values are calculated based on thickness of the layer which is 0.5mm. Epoxy properties are assumed to be isotropic due to lack of data. Contour integral cracks were inserted in the substrates with the seam length equal to the crack length, as shown in Fig. 2(b). Stress intensity factors at the crack fronts were obtained from history outputs at maximum energy release rate criterion for FCG.

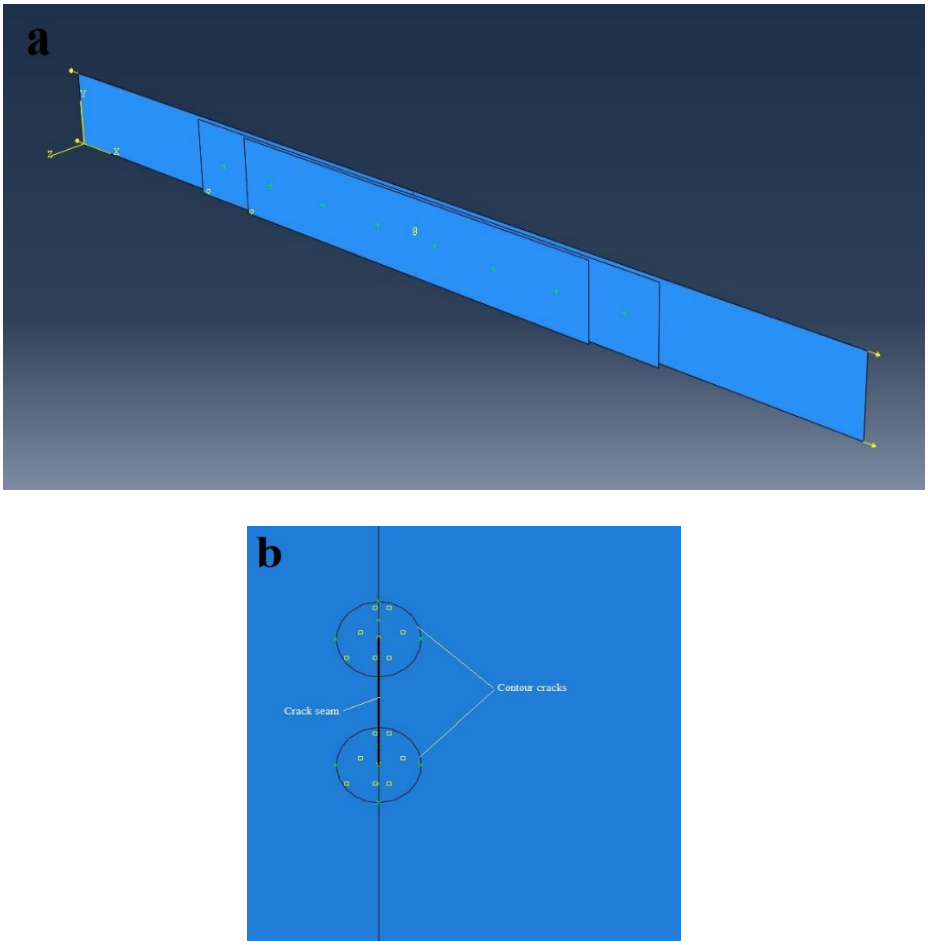

Fig. 2 (a) Isometric view of riveted joint model in the graphical user interface of ABAQUS with point based fasteners, and (b) detail of the insertion of a contour integral crack in the joint model.

3. Results and Discussions

Table 4 shows the fatigue life of the substrate plate with various crack lengths, as obtained from FRANC3D. A null stress ratio is applied for all crack sizes. Fig. 3 shows the stress intensity factors as obtained with FRANC3D for three contours of FCG and various crack lengths at applied stress of 93.6 and 140 MPa. The zeroth contour corresponds to the initial stress intensity factor without growth and the later three contours are the stress intensity factors after initiation of FCG. Fig. 4 shows the crack propagation of 5mm initial crack at applied stress of 93.6 MPa. The latter values for the substrate plates are below the fracture toughness K_C of AA 2024-T3 (see Table 3).

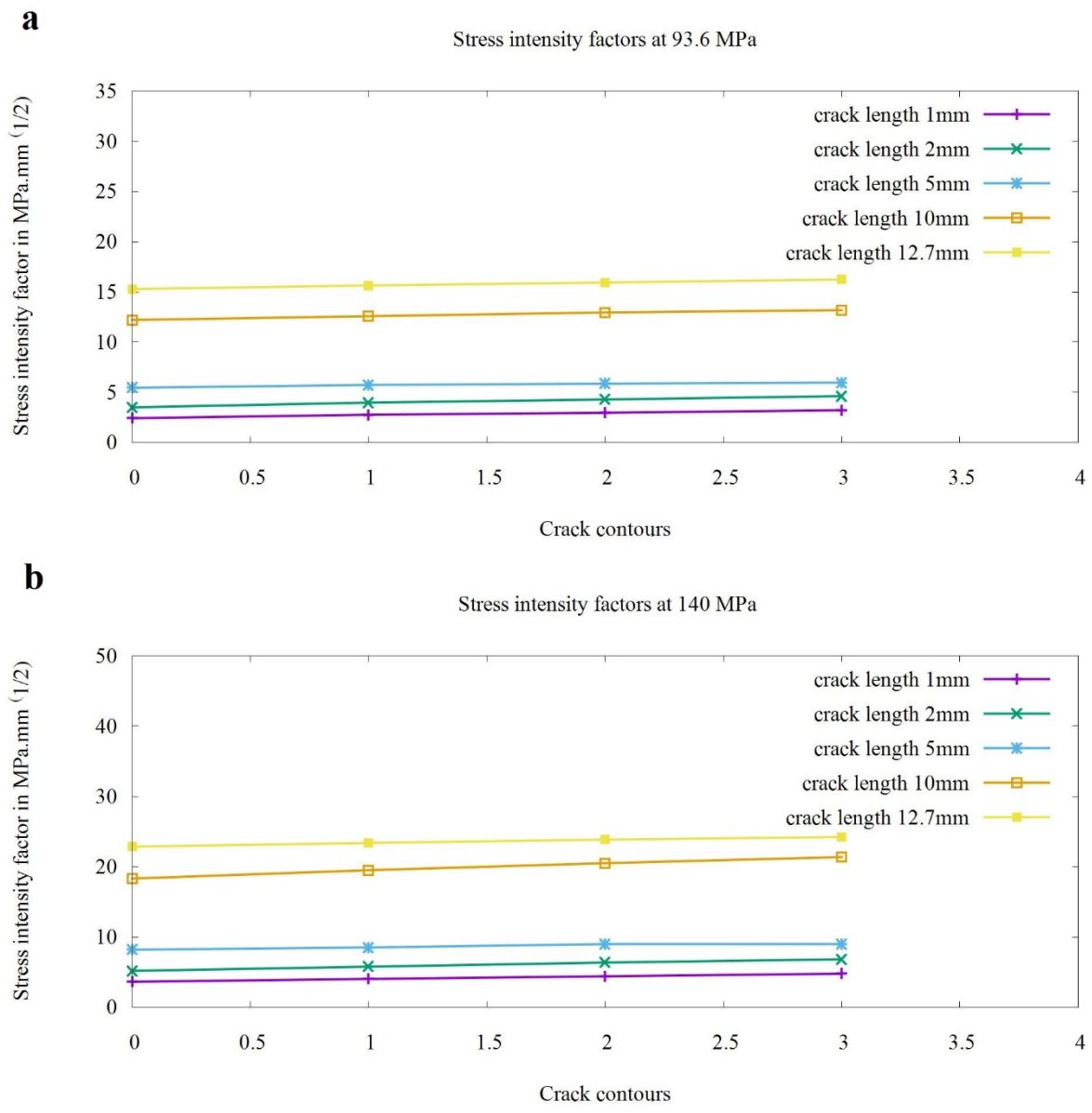

Fig. 3 Stress intensity factors for different crack lengths and contours for a tension of (a) 93.6 MPa and (b) 140 MPa.

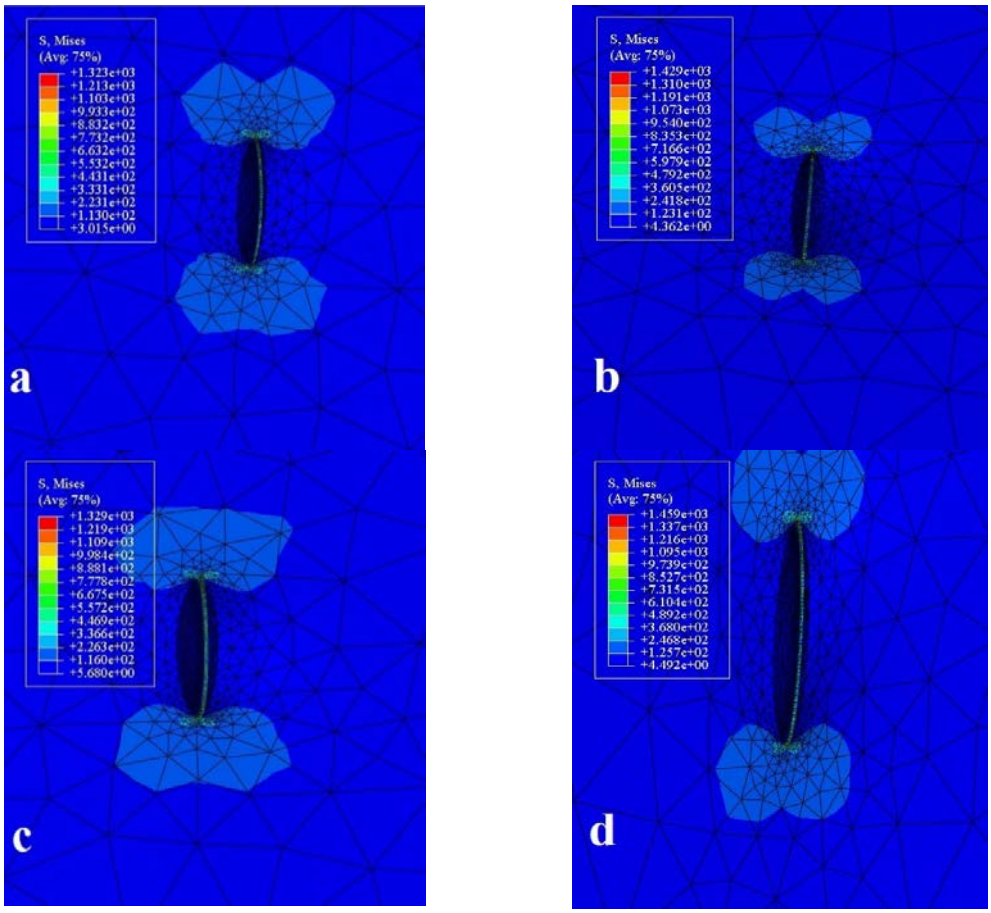

Fig. 4 Crack propagation for initial crack size 5mm for a tension of 93.6 MPa (a) static analysis (b) contour 1 (c) contour 2 and (d) contour 3

Table 4. Fatigue life for AA 2024-T3 substrate plate for different crack length and stresses

Crack length (mm)	Fatigue Life (N_f) for 93.6 MPa	Fatigue life (N_f) for 140 MPa
1	314362	48193
2	178451	30024
5	14447	3670
10	1206	616
12.7	576	126

Average aircraft structures are designed for 50000-100000 flights. Based on the crack size, the number of cycles to failure can be calculated. The repairs with doubler plates should arrest further FCG in the substrate plate. FRANC3D is used to obtain the number of cycles to failure and ABAQUS is used to obtain the stress intensity factors for the studied joint configurations. Repaired substrates are further modelled and analysed in FEA tool ABAQUS. Fig. 5 shows the obtained stress intensity factors for the riveted and bonded joints, stressed at 93.6 and 140 MPa.

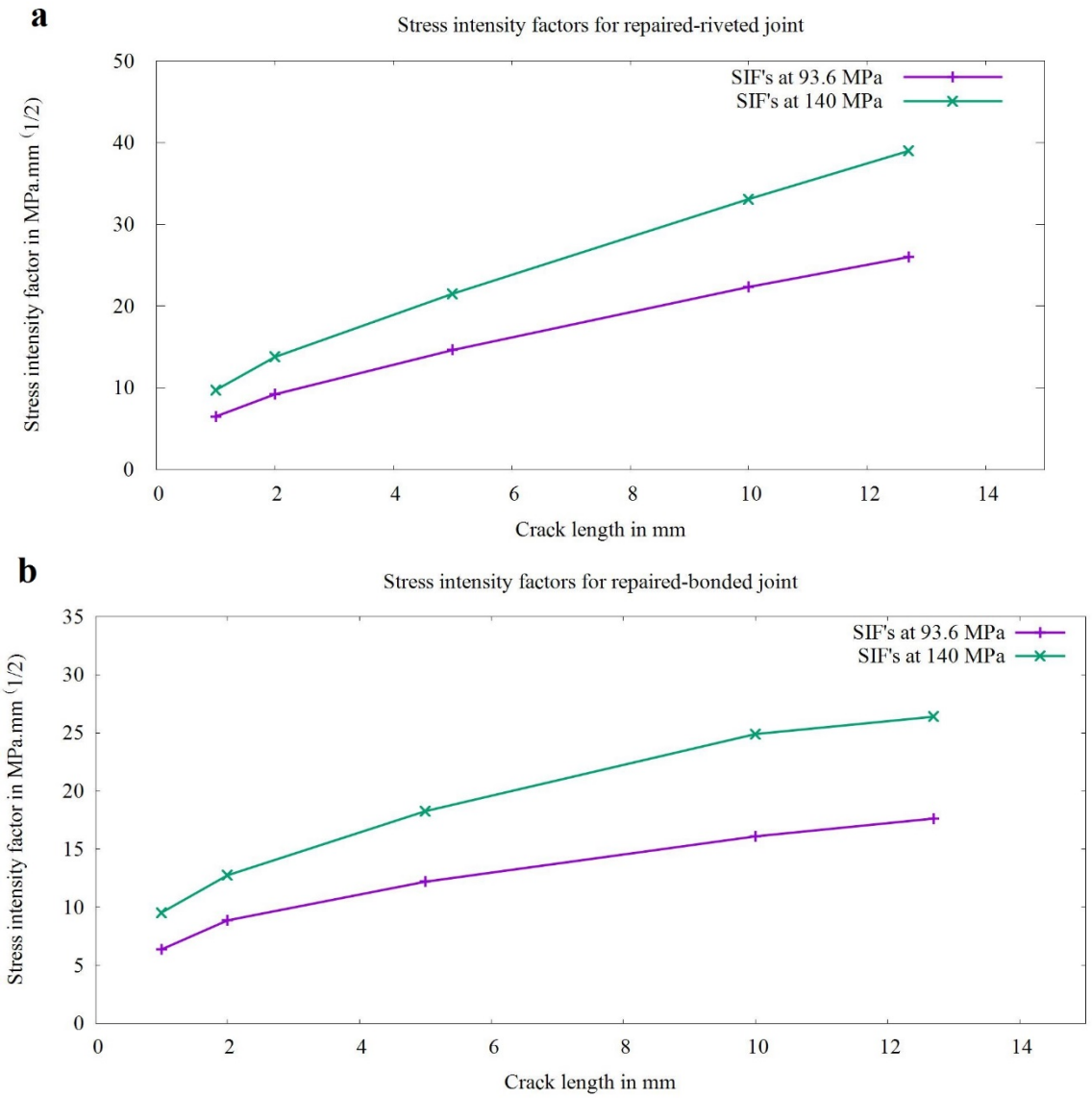

Fig. 5 Stress intensity factors for (a) riveted joint of aluminium alloy (AA) doubler with AA substrate plate, and (b) bonded joint of AA doubler with AA substrate plate.

The results from ABAQUS show that bonded joints result in lower stress intensity factors than riveted joints for crack lengths higher than 2mm. For the cracks of 1 and 2mm, the stress intensity factors at the crack fronts for the riveted and bonded joints are nearly equal. At a stress of 93.6 MPa, the bonded joints have stress intensity factor of maximum 17.63 MPa.mm$^{0.5}$, whereas for the riveted joints the maximum was 26 MPa.mm$^{0.5}$. It is remarkable the difference between the stress intensity factors given by FRANC3D and ABAQUS. This is because they use different FCG criterion; namely, FRANC3D uses a quasi-static power law to compute FCG, while ABAQUS uses a maximum energy release rate criterion.

4. Conclusions

The fatigue life of AA 2024-T3 plates with different crack lengths was investigated using FRANC3D. In addition, cracked AA plates were repaired with riveted and adhesive bonded joints, and the stress intensity factors for these repairs for various crack lengths and loading conditions were studied with the FEA tool ABAQUS. The conclusions from the numerical analysis of the studied repair joints are:

- Repairs made with riveted joints may arrest or reduce the crack growth in substrates but fastener holes in the substrate have high stress concentrations.
- Repairs made with bonded joints show lower stress intensity factors compared with those made with riveted joints.
- The stress intensity factors at the crack front are nearly equal for the riveted and bonded joint configurations for a crack length of 2mm. This suggests that cracks with length under 2mm cause no significant differences in the behaviour of the stress intensity factor for riveted and bonded joint configurations.
- The stress-intensity factor exceeds the critical stress intensity value for repaired-riveted joint with crack length of 12.7mm at 140 MPa, implies the failure is static.
- Load transfer in bonded joints is smoother and has lower secondary bending.

Further experimental investigations on repairs made with riveted and bonded joints are on-going with the purpose of validating the numerical results.

References

[1] Yan Y, Wen W D, Chang F K and Shyprykevich P 1999 *Compos. Part. A* **30** pp 1215-29

[2] Minguez J M and Vogwell J 2006 *Eng. Fail. Anal.* **13** pp 1410-21

[3] Oskouei R H, Keikhosravy M and Soutis C 2009 *Proc. Inst. Mech. Eng. Part. G J. Aerosp. Eng.* **223** p 863

[4] Chakherlou T N and Vogwell J 2003 *Eng. Fail. Anal.* ***10*** 2003 pp 13-24

[5] Chakherlou T N, Oskouei R H and Vogwell J *Eng. Fail. Anal.* ***15*** 2008 pp 563-74

[6] Chakherlou T N, Mirzajanzadeh M, Abazadeh B and Saeedi k *Eur. J. Mech. A Solid **29*** 2010 pp 675-82

[7] Iyer k, Hu S J, Brittman F L, Wang P C, Hayden D B and Marin S P *Fatigue Fract. Eng. Mater. Struct.* **28** 2010 pp 997-1007

[8] Rijck J J M, Homan J J, Schijve J and Benedictus R *Int. J. Fatigue* **29** 2007 pp 2208-18

[9] Skorupa M, Skorupa A, Machneiwicz T and Korbel A *Int. J. Fatigue* **58** 2014 pp 209-17

[10] Esmaeili F, Chakherlou T N and Zehsaz M *Mat. And Design* **59** 2014 pp 430-38

[11] Carter Ralph W, Steven Johnson W, Andrew M and James C *Int. J. Fatigue* **29** 2007 pp 1319-27

[12] Ferjaoui A, Yue T, Abdel Wahab M and Hojjati-Talemi R *Int. J. Fatigue* **73** pp 66-76

[13] Hojjati Talemi R and Abdel Wahab M *Tribology Int.* **60** pp 176-186

[14] Inman M E, Kelly R G and Williard R S *Proc. FAA-NASA symposium on the continued Airworthiness of Aircraft Structures (Virginia, USA)* p 129

[15] Wallace W, Hoeppner D W and Kandachar P V *AGARD Corrosion handbook I* 1985 p 278

[16] Pantelakis Sp G, Vassilas N I and Daglaras *Metall* **47** 1993 pp 135-41

[17] Pantelakis Sp G, Daglaras P G and Apostolopoulos Ch Alk *J. Theor. Appl. Fract. Mech* **33** 2000 p 117

[18] Papnikos P and Kermanidis Al Th *Proc. 4th Int. Conf. on new challenges in Mesomechanics (Denmark)* 2002

[19] Smiyan O D, Coval M V and Melekhov R K *Soviet Mater. Sci* **19** 1983 pp 422-30

[20] Charitidou E, Papapolymerou G, Haidemenopooulos G and Hassiotis N *Script. Mater.* **41** 1999 p 41

[21] Petroyiannis P V, Kermandis Al Th, Kamoutsi E, Pantelakis G Sp, Bontizoglou and Haidemenopoulos G V*Fract. Eng. Mater. Struct.* **28** pp 565-574

[22] Baker A A and Jones R *Bonded Repair of Aircraft Structures* 1988 chapter 4-5

[23] Rose L R F *Int. J. Solids Structures* **17** 1981 pp 827-38

[24] Ratwani M M *J. Eng. Mat. And Tech.* **100** 1978 pp 46-51

[25] Banea M D and da Silva L F M *Proc. IMECHE Vol. 223 Part I, J. Mater. Design and appl.* 2009

[26] Baker A *Compos. Struct.* **47** 1999 pp 431-43

[27] Koutsourelakis P S, Kuntiyawichai K and Schuëller G I *Eng. Fract. Mech.* **73** 2006 pp 1202-19

[28] Harman A B and Rider A N *Int. J. Adh. & Adh.* **44** 2013 pp 144-56

[29] Kaiser Aluminium Frabricated Products, USA, *Material properties AA 2024-T3* 2016

[30] Swift T *ASTM STP 842* 1984 pp 69-107